

This is the author's final, peer-reviewed manuscript as accepted for publication (AAM). The version presented here may differ from the published version, or version of record, available through the publisher's website. This version does not track changes, errata, or withdrawals on the publisher's site.

## Understanding the role of designed solid acid sites in the low-temperature production of $\epsilon$ -Caprolactam

Matthew E. Potter, Stephanie Chapman,  
Alexander J. O'Malley, Alan Levy, Marina Carravetta,  
Thomas M. Mezza, Stewart F. Parker, and Robert Raja

### Published version information

This is the peer reviewed version of the following article:

**Citation:** ME Potter et al. "Understanding the role of designed solid acid sites in the low-temperature production of  $\epsilon$ -Caprolactam." ChemCatChem vol. 9, no. 11 (2017): 1897-1900.

**DOI:** [10.1002/cctc.201700516](https://doi.org/10.1002/cctc.201700516).

Which has been published in final form at [10.1002/cctc.201700516](https://doi.org/10.1002/cctc.201700516). This article may be used for non-commercial purposes in accordance With Wiley-VCH Terms and Conditions for self-archiving.

Please cite only the published version using the reference above. This is the citation assigned by the publisher at the time of issuing the AAM. Please check the publisher's website for any updates.

This item was retrieved from **ePubs**, the Open Access archive of the Science and Technology Facilities Council, UK. Please contact [epubs@stfc.ac.uk](mailto:epubs@stfc.ac.uk) or go to <http://epubs.stfc.ac.uk/> for further information and policies.

# Understanding the Role of Designed Solid Acid Sites in the Low-Temperature Production of $\epsilon$ -Caprolactam

Matthew E. Potter,<sup>[a]</sup> Stephanie Chapman,<sup>[a]</sup> Alexander J. O'Malley,<sup>[b, c]</sup> Alan Levy,<sup>[d]</sup> Marina Carravetta,<sup>[a]</sup> Thomas M. Mezza,<sup>[e]</sup> Stewart F. Parker,<sup>[f]</sup> and Robert Raja\*<sup>[a]</sup>

Modern society is placing increasing demands on commodity chemicals, driven by the ever-growing global population and the desire for improved standards of living. As the polymer industry grows, a sustainable route to  $\epsilon$ -caprolactam, the precursor to the recyclable nylon-6 polymer, is becoming increasingly important. To this end, we have designed and characterized a recyclable SAPO catalyst using a range of characterization techniques, to achieve near quantitative yields of  $\epsilon$ -caprolactam from cyclohexanone oxime. The catalytic process operates under significantly less energetically demanding conditions than other widely practiced industrial processes.

The nylon industry has been valued at 14 billion USD for 2019,<sup>[1, 2]</sup> making the synthesis of  $\epsilon$ -caprolactam, the precursor for recyclable nylon-6 fibers, of great relevance. The acid-catalyzed Beckmann rearrangement of cyclohexanone oxime to  $\epsilon$ -caprolactam conventionally<sup>[3]</sup> employs aggressive reagents, thereby compromising the sustainability from an environmental and ecological perspective. This can be circumvented by a vapor-phase process with a solid-acid catalyst,<sup>[4–6]</sup> but the high temperatures required to keep both lactam and oxime in

the gas-phase make this process energy intensive. A wide-range of catalysts have been investigated, however most suffer from lower selectivities and limited catalyst stability, owing to the high-temperatures employed.<sup>[4–13]</sup>

The liquid-phase Beckmann rearrangement employs considerably lower temperatures than the vapor-phase process, reducing energy consumption, though typically at the cost of conversion and yields, often requiring considerable solvent quantities for product separation.<sup>[14–16]</sup> As such, we recognize the need for a heterogeneous catalyst, which comprises a targeted, active site (single-site) that possesses the desired acid-strength to deliver high catalytic activities and selectivities under benign conditions. Aluminophosphates (AIPOs) are prime candidates, as their porous architectures offer high selectivity, akin to zeolites. Moreover, incorporating small quantities of dopants into an AIPO creates Brønsted acid sites, that can vary in strength, depending on the synthesis procedure and framework topology.<sup>[17, 18]</sup> A comparison of silicon-substituted AIPOs (SAPOs) and other porous structures emphasizes the need for a carefully designed catalyst (Figure 1, Table S1). SAPO-37 shows great potential under these conditions, but a more general trend between pore size and activity is observed for other SAPO materials. In contrast, mesoporous materials offer little impedance to molecular diffusion, but are far inferior in performance compared to SAPOs, owing to the lack of Brønsted acidity.<sup>[19, 20]</sup>

Magic angle spinning (MAS) <sup>29</sup>Si NMR was used to probe the silicon environments to elucidate the differences in catalytic

[a] Dr. M. E. Potter, S. Chapman, Dr. M. Carravetta, Prof. R. Raja School of Chemistry  
University of Southampton  
Southampton, SO17 1BJ (UK)  
E-mail: R.Raja@soton.ac.uk

[b] Dr. A. J. O'Malley  
UK Catalysis Hub, Research Complex at Harwell,  
Science and Technology Facilities Council, Rutherford Appleton  
Laboratory Harwell Science and Innovation Campus, OX11 0QX (UK)

[c] Dr. A. J. O'Malley  
Cardiff Catalysis Institute, School of  
Chemistry Cardiff University  
Cardiff, CF10 3AT (UK)

[d] Dr. A. Levy  
Honeywell Int.  
101 Columbia Rd  
Morristown, NJ 07962 (USA)

[e] Dr. T. M. Mezza  
UOP LLC  
50 E. Algonquin Rd.  
Des Plaines, IL 60016 (USA)

[f] Dr. S. F. Parker  
ISIS Neutron and Muon Facility, Science and Technology Facilities  
Council, Rutherford Appleton Laboratory  
Harwell Science and Innovation Campus, OX11 0QX (UK)

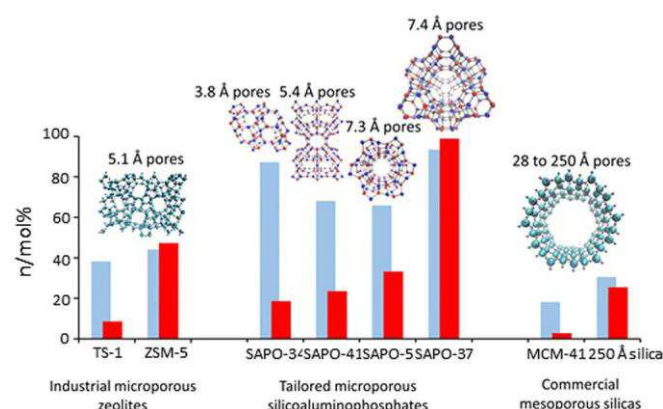


Figure 1. Contrasting the catalytic activity and selectivity of conventional mi-croporous and mesoporous materials alongside that of the SAPOs for the liquid-phase Beckmann rearrangement of cyclohexanone oxime at 130 8C (7 h) blue =caprolactam selectivity, red =conversion of cyclohexanone oxime (see also Table S1).

behavior between the similar pore-sized (though differing framework topology) SAPO-5 and SAPO-37 catalysts. The  $^{29}\text{Si}$  NMR spectrum of SAPO-37 shows a broad peak at  $\sim 91$  ppm (Figure S1), diagnostic of isomorphous substitution of Si for P in the framework (notably  $\text{Si}(\text{OAl})_4$  and  $\text{Si}(\text{OAl})_3(\text{OSi})$ ) are poorly-resolved owing to the moisture-sensitivity of SAPO-37.<sup>[21]</sup> In contrast, SAPO-5 shows a broad peak centered at  $\sim 101$  ppm, indicative of silicon zoning through  $\text{Si}(\text{OAl})_2(\text{OSi})_2$ ,  $\text{Si}(\text{OAl})(\text{OSi})_3$ ,  $\text{Si}(\text{OSi})_4$  species and extra framework sites.<sup>[21, 22]</sup> This produces fewer, but stronger, Brønsted acid sites on the periphery of silicon zones.<sup>[21, 22]</sup> It is therefore highly likely that the isolated acid sites observed in the SAPO-37 catalyst are more active than the acid sites associated with silicon islands.

To investigate the interactions between the SAPO-37 framework and cyclohexanone oxime, inelastic neutron scattering (INS) spectroscopy was employed. INS spectra are dominated by vibrations involving motion of hydrogen, other elements having only a minor contribution. The framework is transparent to neutrons throughout the diagnostic fingerprint region ( $0\text{--}1800\text{ cm}^{-1}$ ), allowing the oxime and lactam to be probed as a physical mixture (10 % cyclohexanone oxime and 90 % SAPO-37, Figure 2). At 363 K the spectra align closely with the bulk oxime, suggesting a physical mixture of catalyst and the oxime substrate. This suggests the substrate has not properly adsorbed/entered the pores. Heating through a range of temperatures shows a progression to bands associated with the caprolactam, which is particularly noticeable at 393 K to 403 K, highlighting the significant potential of solid SAPO-37 as a low-temperature (250 °C lower than conventional methods), liquid-phase Beckmann rearrangement catalyst.

To further optimize the SAPO-37 catalyst, a range of Si:P gel ratios were investigated (Table S2). It was revealing that minimal amounts of Si in the synthesis gel (ratio of 0.11) promotes the formation of the more thermodynamically stable AFI phase. However SAPO-37(0.21), (0.42) and (0.63) showed near-identical powder-XRD patterns, confirming their crystallinity and phase-purity (Figure S2). Moreover, unit cell parameters were found to increase with increased silicon content, indicative of isomorphous substitution of  $\text{Si}^{\text{IV}}$  for  $\text{P}^{\text{V}}$ .<sup>[22]</sup> The textural properties of the three SAPO-37 catalysts were in agreement with each other and with literature values (Figures S3–S5).<sup>[23]</sup> 2D MAS  $^{29}\text{Si}$  NMR showed the effect of silicon loading on the distribution of silicon environments (Figures 3 A-C and S1, S6 and S7). For increased resolution, experiments were performed under a constant flow of dry nitrogen for drive, purge and bearing. As a result, individual peaks at  $\sim 98$  and  $\sim 93$  ppm were resolved and assigned as  $\text{Si}(\text{OAl})_3(\text{OSi})$  (from 5-silicon islands) and the isolated  $\text{Si}(\text{OAl})_4$  weak Brønsted acid species, respectively. The latter typically manifests between  $\sim 89$  and  $\sim 92$  ppm, but the anhydrous nature of the experiment is believed to alter the peak position slightly. The spectra show that higher silicon loadings favor Si-O@Si bonding through an increase in the  $\sim 98$  ppm signal ( $(\text{Si}(\text{OAl})_3(\text{OSi}))$ <sup>[22]</sup> relative to the signal at  $\sim 93$  ppm ( $\text{Si}(\text{OAl})_4$ ). Evidence for silicon clustering is seen at  $\sim 101$ ,  $\sim 104$  and  $\sim 108$  ppm in the SAPO-37(0.42) and (0.63) spectra, corresponding to  $\text{Si}(\text{OSi})_2(\text{OAl})_2$ ,  $\text{Si}(\text{OSi})_3(\text{OAl})$  and

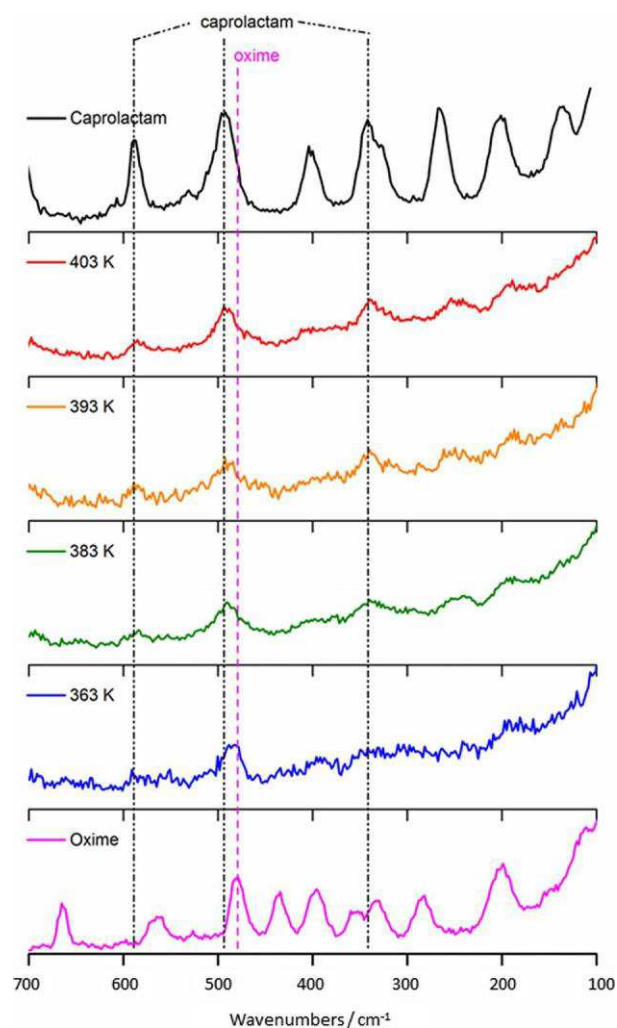


Figure 2. Variations in the INS vibrational spectrum of a cyclohexanone oxime/SAPO-37 mixture on increasing temperature.

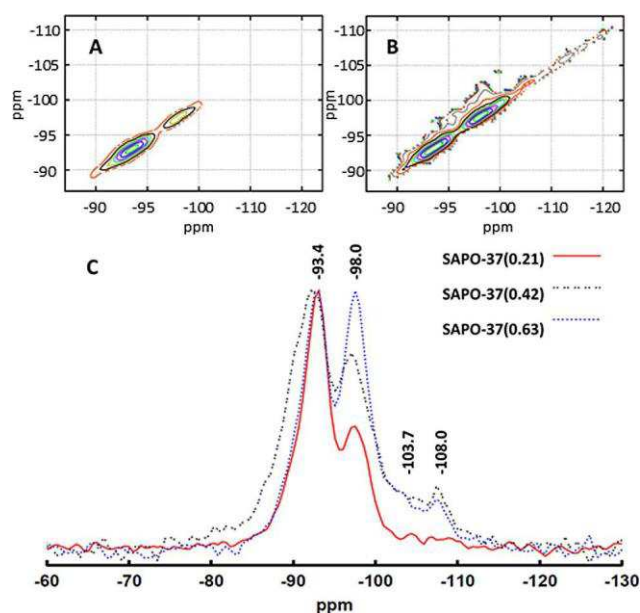


Figure 3. A and B) 2D MAS  $^{29}\text{Si}$  NMR under  $\text{N}_2$  of SAPO-37(0.21), SAPO-37(0.63) and C) 1D MAS  $^{29}\text{Si}$  NMR of SAPO-37 containing different Si:P ratios.

Si(OSi)<sub>4</sub> species, respectively, in both the 1D and 2D NMR spectra.<sup>[21, 22]</sup> These findings suggest that a lower silicon loading is necessary to promote the Si(OAl)<sub>4</sub> environment, which is crucial for creating the desired, isolated catalytically-active sites, that are fundamental for the low-temperature Beckmann rearrangement. Despite variations in the <sup>29</sup>Si NMR, both <sup>27</sup>Al and <sup>31</sup>P NMR signals were commensurate, showing predominantly Al(OP)<sub>4</sub> and P(OAl)<sub>4</sub> signals (Figures S6 and S7), thereby vindi-cating the overall structural integrity of the SAPO-37 catalysts.

Acid strength is also of fundamental importance in the Beckmann rearrangement.<sup>[14, 16]</sup> Active sites must be sufficiently strong to form the lactam, yet weak enough to permit its subsequent desorption from the catalyst (Scheme S1).<sup>[16]</sup> Temperature programmed desorption (TPD) experiments show that SAPO-37(0.21) and (0.42) possess a similar number of acid sites (0.93 and 0.87 mmol g<sup>-1</sup>, respectively), though the SAPO-37(0.63) system had fewer (0.76 mmol g<sup>-1</sup>, Figures 4 and Table S3). Lower silicon loadings favor a greater number of weaker acid sites (200–400 8C), whilst increasing the silicon loading promotes the formation of stronger acid sites (400–500 8C). These observations further reinforce our earlier NMR findings.<sup>[24, 25]</sup> The TPD values obtained for the SAPO-37(0.21) catalyst also correlate well with the theoretical total acidity, (Schemes S2 and S3, Table S2 and S4) calculated from the inductively coupled plasma atomic emission spectroscopy and NMR data (0.98 mmol g<sup>-1</sup>).

The FTIR spectra of SAPO-37 show bands at 3641 and 3575 cm<sup>-1</sup> corresponding to the hydroxyls in the supercage

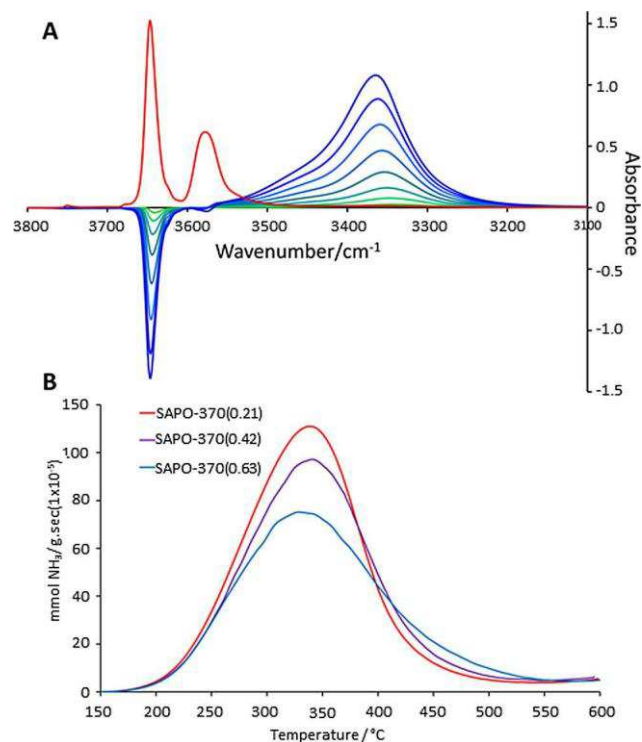


Figure 4. A) The influence of CO binding on the hydroxyl region of SAPO-37(0.21) with increasing CO<sub>2</sub> quantities (green to blue) whereas B) NH<sub>3</sub>-TPD data reveals a greater fraction of strong acid sites with increasing Si:P ratios in SAPO-37 catalysts.

and sodalite cages of the faujasitic framework, respectively (Figure 4 and Figure S8). The intensity of the 3641 cm<sup>-1</sup> band shows that SAPO-37(0.21) and (0.42) possess similar quantities of hydroxyl groups, in contrast to SAPO-37(0.63) (Figure S9-S11, Table S5). Low temperature CO adsorption showed only the 3641 cm<sup>-1</sup> band, which was reduced significantly as a new band appeared at 3330 cm<sup>-1</sup>, confirming interaction with the CO. The inflection at 3450 cm<sup>-1</sup> is attributed to CO interacting with P-OH bonds, and proton migration from the sodalite cage to the supercage, making the protons accessible. The degree of the displacement of the hydroxyl band on CO adsorption is associated with the average overall acid strength of the material, which, in agreement with TPD data, increased with silicon loading (Figures S8–S11, Table S5). The CO band at 2180–2160 cm<sup>-1</sup>, which can be used to quantify total acidity, highlights the similarities between SAPO-37(0.21) and (0.42), whereas SAPO-37(0.63) possesses fewer acid sites. From this data, the proton affinity was calculated as 1155, 1152 and 1146:

(5) kJ mol<sup>-1</sup> for SAPO-37(0.21), (0.42) and (0.63), respectively,<sup>[26]</sup> in agreement with literature values.<sup>[27]</sup> Collidine was subsequently employed as a similar-sized probe to cyclohexanone oxime, to investigate accessibility to the active site. The bands at 1652 and 1637 cm<sup>-1</sup> (O-H...N interactions, Figures S12-S15, Table S6), were quantified at different temperatures to probe acid strength. This data ratifies the observation that a lower silicon content favors more weak acid sites. Thus, by using a variety of characterization techniques, we have shown that SAPOs can be prepared with comparable physical characteristics but, by reducing silicon content, it is possible to promote the formation of isolated, weak Brønsted acid sites that are better suited for the Beckmann rearrangement. In the liquid-phase Beckmann rearrangement, variations in lactam yield and turn-over number (TON) between the various SAPO-37 catalysts, is apparent (Table 1, S7, and Figures S16–S39). As SAPO-37(0.21) and (0.42) possess a similar quantity of acid sites, the improved selectivity for caprolactam in SAPO-37(0.21) can be attributed to the targeted weaker acid sites (Table 1). These weaker acid sites are known to enable faster lactam desorption in the vapor-phase process,<sup>[4–6]</sup> and we believe, they play a similar role in the SAPO-37(0.21) catalyst. Above 170 8C, temperature was found to have negligible effect on reaction rate, indicating that the process becomes mass-transfer limited (Table S7). Arrhenius analysis provides further confirmation that the production of caprolactam is first-order, in agreement with the mechanism postulated for the Beckmann rearrangement.<sup>[11, 26, 28]</sup>

The activation energy for SAPO-37(0.21) is lower than the SAPO-37(0.42) and (0.63) catalysts (Figure S40, Table S8) which, at 50 kJ mol<sup>-1</sup>, is in good agreement with work performed in the vapor-phase,<sup>[11, 28]</sup> (Scheme S4), suggesting that the reaction proceeds through an analogous pathway in the liquid-phase.

As water promotes site deactivation and cyclohexanone production,<sup>[16]</sup> the Beckmann rearrangement was further optimized under anhydrous conditions (Table 1, Figure S41–S44) to maximize conversion and selectivity (Table 1 and Table S9) to near-quantitative yields of *e*-caprolactam. Benzonitrile is a relatively non-polar solvent and was chosen for this study, as its high boiling facilitates facile separation of caprolactam. We

Table 1. Summary of catalytic results for the low-temperature Beckmann rearrangement of cyclohexanone oxime to  $\epsilon$ -caprolactam (conditions as per Figure 1).

System	Time [mins]	Conversion [mol %]	TON [mol mol <sup>-1</sup> ]	e-caprolactam selectivity <sup>[a]</sup> [mol %]	Total Acid quantity <sup>[b]</sup> [mmol g <sup>-1</sup> ]	Degree of site isolation <sup>[c]</sup> [%]	Weak +Medium acid sites <sup>[d]</sup> [au mg <sup>-1</sup> ]
SAPO-37(0.21) Anhydrous	180	93.4	7.9	97.8	0.93	71	3.76
	420	99.8	8.4	97.8			
SAPO-37(0.21) Wet	180	89.3	7.5	96.0	0.93	71	3.76
	420	98.9	8.3	93.5			
SAPO-37(0.42) Wet	180	89.8	2.9	93.3	0.87	48	3.11
	420	98.8	3.2	90.3			
SAPO-37(0.63) Wet	180	90.4	2.4	90.9	0.77	41	2.80
	420	99.8	2.6	88.4			

[a] By-products include cyclohexanone and products from solvent-oxime reactions. [b] From NH<sub>3</sub>-TPD. [c] From curve fitting <sup>29</sup>Si MAS NMR. [d] From collidine FTIR.

further confirmed the heterogeneity and stability of the SAPO-37 catalyst, which reveals sustained levels of conversion and selectivity, after several recycles (Figure S45).

In conclusion, this work represents a significant advancement in understanding how industrially attractive yields of  $\epsilon$ -caprolactam might be achieved through a liquid-phase Beckmann rearrangement. We have shown how the design approach can be suitably modulated to facilitate the generation of isolated active sites, which has a direct impact on the nature and strength of the resulting solid-acid sites. Catalytic and spectroscopic protocols have been deployed to further elucidate the relationship between the nature and strength of acidic active sites and the ensuing efficiency of the SAPO-37 catalyst (Table 1) in the low-temperature Beckmann rearrangement, which affords near-quantitative yields of  $\epsilon$ -caprolactam.

## Acknowledgements

The UK Catalysis Hub is kindly thanked for resources and support provided through our membership of the UK Catalysis Hub Consortium. We thank the STFC Rutherford Appleton Laboratory and ISIS Pulsed Neutron and Muon Source for access to neutron beam facilities. The UK Catalysis Hub is funded by EPSRC (Engineering and Physical Sciences Research Council) through grants EP/K014706/1, EP/K014668/1, EP/K014854/1, EP/K014714/1 and EP/M013219/1. The EPSRC also funded the Centre for Doctoral Training Scheme with grant no. EP/G036675/1. The project was also funded by the Science and Technologies Facilities Council and ISIS Pulsed Neutron Muon Source. MEP and SC also acknowledge Honeywell LLC for studentship.

**Keywords:** beckmann rearrangement · aluminophosphates · heterogeneous catalysis · solid acid · sustainable chemistry

[1] "Nylon—A global strategic business report" Global industry analysts inc., 2010.

[2] "World analysis—Nylon engineering resins" IHS chemicals, <http://www.ihs.com/products/chemical/planning/world-petro-analysis/nylon-engineering-resins.aspx>.

[3] E. De Decker, J. Oostvogels, G. Van Wauwe, G. Neubauer, (BASF Aktien-gesellschaft) US4804754 A, 1989.

- [4] W. F. Hölderich, J. Roseler, G. Heitmann, A. T. Liebens, *Catal. Today* 1997, 37, 353 – 366.
- [5] G. Bellussi, C. Perego, *CATTECH* 2000, 4, 4 – 16.
- [6] a) H. Ichihashi, M. Kitamura, *Catal. Today* 2002, 73, 23 – 28; b) H. Ichihashi, H. Sato, *Appl. Catal. A* 2001, 221, 359 – 366.
- [7] J. Kim, W. Park, R. Ryoo, *ACS Catal.* 2011, 1, 337 – 341.
- [8] H. Kath, R. Glaser, J. Weitkamp, *Chem. Eng. Technol.* 2001, 24, 150 – 153.
- [9] L. Forni, G. Fornasari, C. Giordano, C. Lucarelli, A. Katovic, F. Trifiro, C. Perri, J. B. Nagy, *Phys. Chem. Chem. Phys.* 2004, 6, 1842 – 1847.
- [10] E. Gianotti, M. Manzoli, M. E. Potter, V. N. Shetti, D. Sun, J. Paterson, T. M. Mezza, R. Raja, *Chem. Sci.* 2014, 5, 1810 – 1819.
- [11] J. Sirijaraensre, J. Limtrakul, *ChemPhysChem* 2006, 7, 2424 – 2432.
- [12] N. R. Shiju, M. Anilkumar, W. F. Holdereich, D. R. Brown, *J. Phys. Chem. C* 2009, 113, 7735 – 7742.
- [13] S. Bordiga, P. Ugliengo, A. Damin, C. Lamberti, G. Spoto, A. Zecchina, G. Spano, R. Buzzoni, L. Dalloro, F. Rivetti, *Top. Catal.* 2001, 15, 43 – 52.
- [14] A. B. Fernandez, I. Lezcano-Gonzalez, M. Boronat, T. Blasco, A. Corma, *J. Catal.* 2007, 249, 116 – 119.
- [15] S. Guo, Z. Du, S. Zhang, D. Li, Z. Li, Y. Deng, *Green Chem.* 2006, 8, 296 – 300.
- [16] C. Ngamcharussrivichai, P. Wu, T. Tatsumi, *J. Catal.* 2005, 235, 139 – 149.
- [17] J. M. Thomas, R. Raja, G. Sankar, R. G. Bell, *Nature* 1999, 398, 227 – 230.
- [18] P. A. Barrett, G. Sankar, C. R. A. Catlow, J. M. Thomas, *J. Phys. Chem.* 1996, 100, 8977 – 8985.
- [19] A. Jentys, N. G. Pham, H. Vinek, *J. Chem. Soc. Faraday Trans.* 1996, 92, 3287 – 3291.
- [20] J. Chen, Q. Li, R. Xu, F. Xiao, *Angew. Chem. Int. Ed. Engl.* 1996, 34, 2694 – 2696; *Angew. Chem.* 1995, 107, 2898 – 2900.
- [21] C. S. Blackwell, R. L. Patton, *J. Phys. Chem.* 1988, 92, 3965 – 3970.
- [22] M. E. Potter, M. E. Cholerton, J. Kezina, R. Bounds, M. Carravetta, M. Manzoli, E. Gianotti, M. Lefenfeld, R. Raja, *ACS Catal.* 2014, 4, 4161 – 4169.
- [23] H. B. Mostad, M. Stocker, A. Karlsson, T. Rorvik, *Appl. Catal. A* 1996, 144, 305 – 317.
- [24] R. Wendelbo, D. Akporiaye, A. Andersen, I. M. Dahl, H. B. Mostad, *Appl. Catal. A* 1996, 142, L197 – L207.
- [25] G. Sastre, D. W. Lewis, C. R. A. Catlow, *J. Phys. Chem. B* 1997, 101, 5249 – 5262.
- [26] V. R. R. Marthala, Y. Jiang, J. Huang, W. Wang, R. Glaser, M. Hunger, *J. Am. Chem. Soc.* 2006, 128, 14812 – 14813.
- [27] S. Coluccia, L. Marchese, G. Martra, *Microporous Mesoporous Mater.* 1999, 30, 43 – 56.
- [28] T. Bucko, J. Hafner, L. Benco, *J. Phys. Chem. A* 2004, 108, 11388 – 11397.